Habib Boudaa[1]*, Fethi Saidi*[1]*, Tahar Nateche*[1]*, Mohammed Hadj Meliani*[2*]

FLUID-STRUCTURE INTERACTION OF AN AIRFOIL EQUIPPED WITH AN ACTIVE CONTROL SYSTEM: NUMERICAL SIMULATION AND POSITIONING STUDY

INTERAKCIJA FLUID-KONSTRUKCIJA KRILNOG PROFILA SA AKTIVNIM SISTEMOM KONTROLE: NUMERIČKA SIMULACIJA I STUDIJA POZICIONIRANJA

Originalni naučni rad / Original scientific paper
UDK /UDC:

Rad primljen / Paper received: 10.11.2021

Adresa autora / Author's address:
1) USTO Maritime Engineering Department, Oran, Algeria
2) Hassiba Benbouali University of Chlef, BO. Box 151 Hay salem, Chlef, 02000, Algeria
*email: m.hadjmeliani@univ-chlef.dz

Keywords
- aerodynamic profile
- rotating cylinder
- Solidworks® v. 2018

Ključne reči
- aerodinamički profil
- rotirajući cilindar
- Solidworks® v. 2018

Abstract

A numerical investigation is performed using Solidworks® 2018 (flow-simulation) with results in good agreement with experimental data of the lift coefficient of a Joukowsky profile calculated with the same conditions. The Solidworks is used to study the dynamics for air passing around an aerodynamic profile NACA2415, equipped with rotating cylinder(s). First, the numerical simulation determined the leading-edge of profile, which was the optimum position of the rotating cylinder with an increase of 3 % of CL and diminished to 17 % of CD compared to the basic profile. The second part of the simulation is reserved for the profile equipped with two rotating cylinders, the first cylinder at the leading-edge and the second at 15 % of the chord. This configuration gives the best results with an increase of 74.15 % of CL and diminishes to 12.98 % of CD. Another simulation is launched to consider the influence of diameter variation (Ø) of the rotating cylinder on the CL and CD. This simulation shows that both parameters mark a proportional increase with augmentation of the rotating cylinder diameter until ∅26 mm, as we note a diminishing of CL when CD increases. As a result, Solidworks® regroups all its modules on the same interface (fluid, structure, and others); this code is verified to be available and is used in aeronautical engineering.

Izvod

U radu je prikazano numeričko istraživanje primenom Solidworks® 2018 (simulacija strujanja) sa rezultatima koji se dobro slažu sa eksperimentalnim podacima za koeficijent uzgona profila Joukovskog, za koji je izveden proračun u istim uslovima. Solidworks je korišćen za proučavanje dinamike opstrujavanja vazduha oko aerodinamičkog profila NACA2415, koji se sastoji od rotirajućeg cilindra (ili cilindara). Prvo je numeričkom simulacijom definisana napadna ivica profila, koja predstavlja optimalni položaj rotirajućeg cilindra sa povećanjem CL za 3 % i smanjenjem 17 % za CD, u poređenju sa osnovnim profilom. Drugi deo simulacije obuhvata profil sa dva rotirajuća cilindra, od kojih se prvi cilindar nalazi na napadnoj liniji, a drugi na 15 % tetive profila. Ovom konfiguracijom se postižu najbolji rezultati, sa povećanjem 74,15 % CL i sa smanjenjem CD na 12,98 %. Druga simulacija je izvedena za razmatranje uticaja promene prečnika (∅) rotirajućeg cilindra na CL i CD. Ova simulacija pokazuje da oba parametra rastu proporcionalno sa promenom prečnika rotirajućeg cilindra sve do ∅26 mm, gde primećujemo pad CL pri porastu CD. Kao rezultat, Solidworks® pregrupiše sve svoje module na istu komponentu (fluid, konstrukcija i ostale); ovaj softver je verifikovan i upotrebljava se u aeronautičkom inženjerstvu.

INTRODUCTION

The lift and drag generated are the basic features of the aerodynamic profile and the improvement of its design can positively affect them. Fluid flow on both surfaces of the profile generates lift due to pressure difference. For a positive generated lift, i.e. an upward force, the pressure on the upper-surface must be low relative to the lower-surface of the aerodynamic profile. This pressure difference or gradient can be achieved by varying the angle of attack (AOA) of the symmetrical profile, or by using another asymmetrical profile (the case studied).

The ability to manipulate the flow of a fluid in a passive or active manner and to apply the desired change to a profile leads to the improvement of these aerodynamic characteristics and its structural design /1/, and which will have immense technological importance, in the goal of increasing lift while reducing drag, /2/.

The passive control method consists of a slight change in the geometry of the profile, we can cite, the generators of the vortex (VGx) /3-5/, the sinusoidal leading edge /6, 7/, especially for aviation, we find the hyperlift device /8/ and winglets /9/. Active control methods consist of adding energy to the flow of the fluid, among these methods, the fluid actuators /10/, (giving energy to the flow through air jets), and the plasma actuators /11, 12/ (ionization of air by electrodes). The addition of rotating cylinders on an aerodynamic profile is among the active control methods; its presence in a fluid is subject to the principle of the Magnus effect /13/. This phenomenon is present when a lateral force applied on a rotating cylinder immersed in a fluid (mainly air), this one (cylinder) will be able to generate a lift by creating a pressure difference on its surface, as shown in Fig. 1.

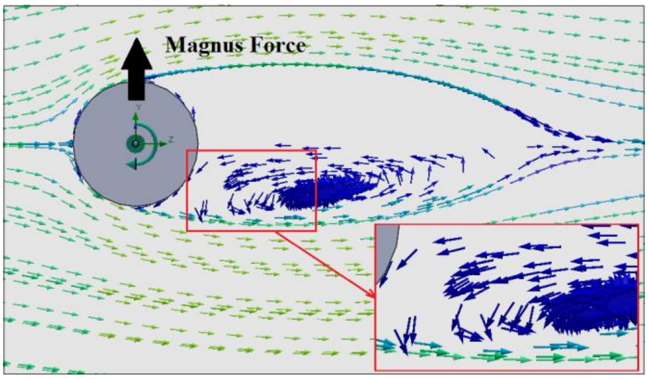

Figure 1. Rotating cylinder in fluid and the Magnus effect.

Studies analysing the flow around a rotating cylinder are less numerous compared to those of the fixed cylinder. The cylindrical structure (cylinder) is placed in a flow of fluid at constant speed, and rotates around its axis with constant angular velocity (ω), Fig. 1. In this field, the flow physics depend on the rotation speed of the cylinder /14/, in addition to the Reynolds number. Most literature studies use the cylinder rotational speeds, $\Phi = (\varnothing\omega)/2V$, expressing the ratio of angular velocity of the cylinder and fluid upstream speed.

The first experiments around a rotating cylinder were conducted by Reid /15/, Tokumaru and Dimotakis /16/, with measurements up to $Re = 1.2\times10^5$. They affirm that the lift coefficient increases with cylinder rotational speed.

In our study, we present three types of rotating cylinder-positioning configurations on a NACA 2415 profile, shown in Fig. 2, Types (i, ii, and iii).

i. One rotating cylinder of diameter $\varnothing$ with angular velocity ω is positioned along the upper-surface of profile NACA 2415. Six (06) configurations are achieved by varying the distance, D. It indicates the position of the cylinder centre relative to the leading-edge, and takes the following values: 0.15C, 0.30C, 0.45C, 0.60C and 0.75C. For the first configuration (0% C), $D = (\varnothing/2) - 1$ mm. This part of the study aims to optimise the position of the cylinder according to the best results obtained from the lift and drag.

ii. Two cylinders have the same diameter $\varnothing$ in rotation with the same angular velocity ω. Five (05) configurations are achieved by varying distance D. It indicates the position of the second cylinder's centre; the first one permanently attached to the leading-edge. Values of D are 0.15C, 0.30C, 0.45C, 0.60C and 0.75C. This second part is devoted to determining a better configuration of two twin rotating cylinders placed on an aerodynamic profile.

iii. A rotating cylinder of diameter $\varnothing$ with an angular velocity ω attached to the leading-edge, varying its diameter, $\varnothing$ = 16, 18, 20, 22, 24, 26, 28 and 30 mm, the centre of the cylinder ($X = \varnothing/2$, $Y = 0$). This last part is reserved to study the influence of diameter variation on the aerodynamic characteristics of the profile. Angular velocity ω varies according to the diameter in equation $\omega = 2V/\varnothing$.

METHODOLOGY

In this study, the aerodynamic characteristics of the NACA 2415 profile are modified by introducing the concept of rotating cylinder on its basic form.

The Solidworks® code used to produce the geometries to be studied, see Fig. 3:

- basic profile NACA2415: chord (C): 250 mm, width 400 mm, see Fig. 3a,
- profile with cylinder of $\varnothing$ = 20 mm and width of 400 mm, see Fig. 3b.

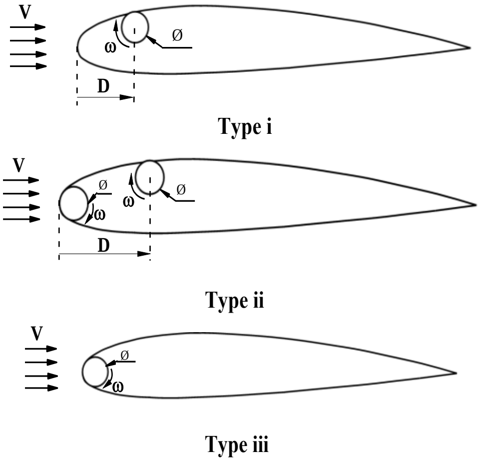

Type i

Type ii

Type iii

Figure 2. Different types of control cylinder configurations.

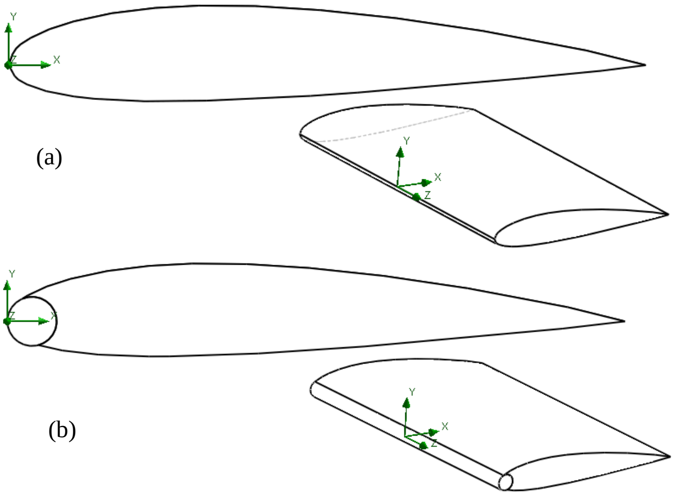

(a)

(b)

Figure 3. Simulated profile geometry.

Computational domain and mesh

Calculations are executed in a rectangular domain 2D, surrounding the profile, Fig. 4. The used mesh is of structured hexa-hydric type of advanced refining, composed of fluid elements in order of 4×10^5 and fluid elements in contact with the solid in the order of 10^5. Figure 5 shows the mesh configuration around the profile.

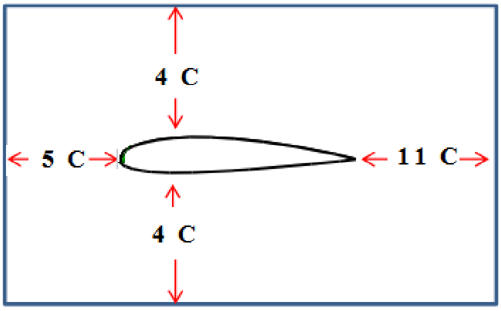

Figure 4. Computational domain with profile.

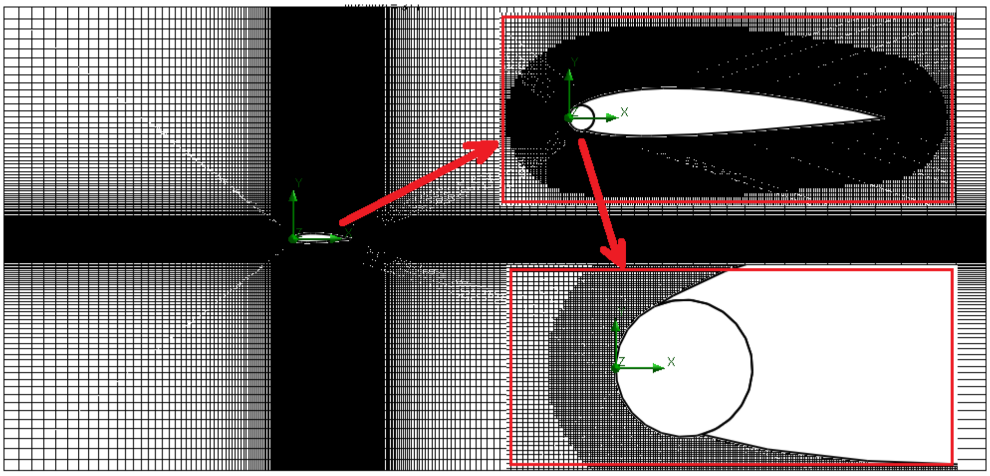

Figure 5. Hexa-hydric mesh.

The geometric specifications that remain the same for all studies are:

- AOA equals zero (0),
- NACA2415 is an asymmetric aerodynamic profile capable of generating at zero-degree (0°) lift,
- the slot between the cylinder wall and the section of the profile are assumed to be zero (to ignore the effect of fluid flow disturbance),
- the surface of the cylinder is above the tangential profile curve of 1.00 ± 0.05 mm, the distance is shown in Fig. 6.

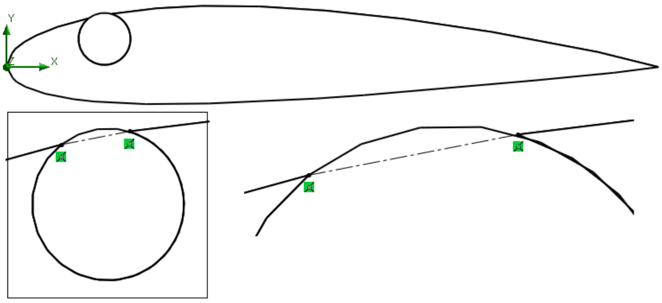

Figure 6. Height between cylinder surface and profile curve.

Initial and boundary conditions

Boundary conditions applied to all regions and ends of the computational domain:

- input: Re = 2.43×10^5,
- output: atmospheric pressure 101325 Pa,
- $\omega = 2\Phi V/\varnothing$,
- $\Phi = 1$ (for the whole study),
- solid walls: ‘upper-surface’, ‘lower-surface’
- turbulence model is $k\varepsilon$.

Validation of the mesh

The used mesh and the efficiency of the Solidworks flow-simulation is validated by the simulation of the experimental study of Modi and Yokomizo /17/. This study is achieved on a symmetrical NACA Joukowsky with chord profile 0.38 m, at angles of attack 0°, 4°, 8°, 10°, and 12°, and Reynolds number of Re = 4.62×10^4.

Figure 7 shows the error between the Solidworks-flow calculation and experimental study, which does not exceed 10 % for the first four angles of attack, and for the 12° stall angle, a gap is noted. In the experiment and in this area of flow, the parameters used to calculate the CL are difficult to measure.

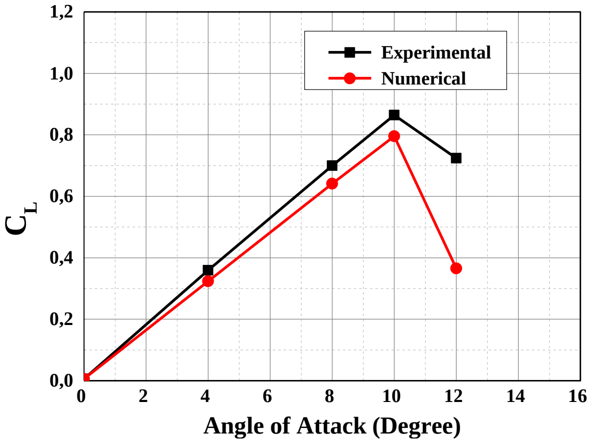

Figure 7. Effect of the angle of attack on CL.

Another study /18/ comparing Ansys CFX and Solidworks 2018 (flow-simulation) under the same conditions shows that the difference of the calculated CD does not exceed 4.29 %.

RESULTS AND DISCUSSION

Influence of rotating cylinder location on the coefficients CL and CD

Figure 8 shows the evolution of CL and CD coefficients as a function of the position of the rotating cylinder on the profile upper-surface. After adaptation, it observed that the rotating cylinder increases the CL by about 3 % and decreases CD by about 17 %, when it is positioned at the leading-edge; for rest of the positions, the adaptations give satisfying results only for drag. The results are compared with the characteristics of the basic profile. The first position is the optimal one and shall be adopted for the continuation of this research.

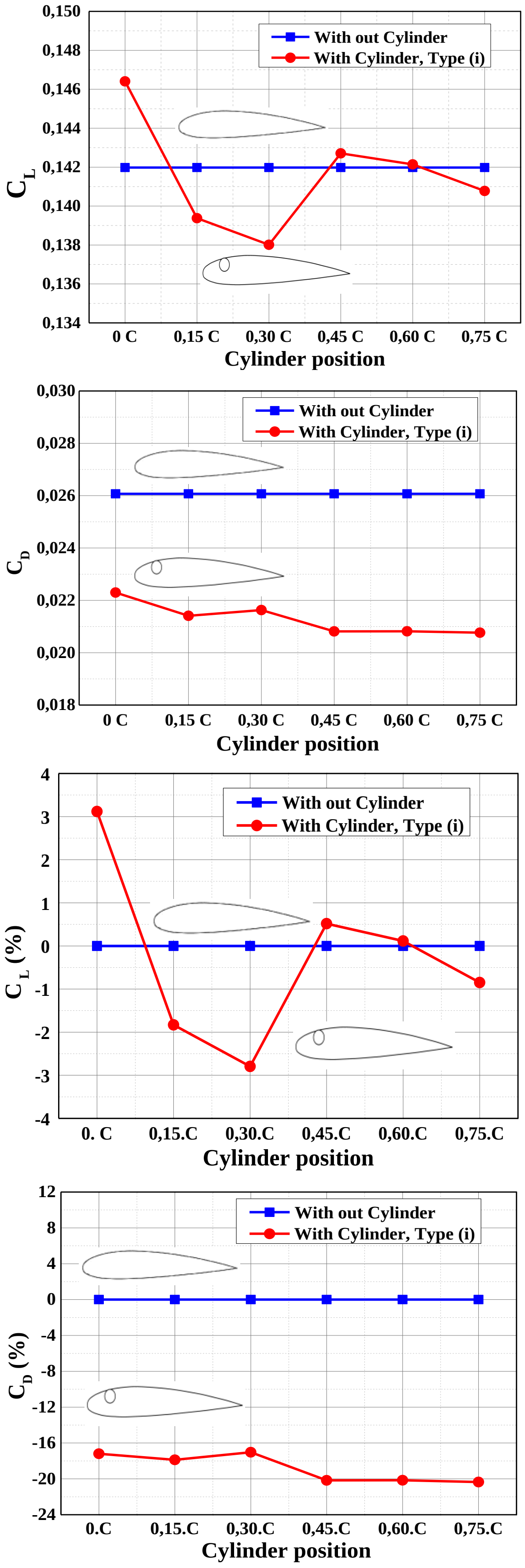

Figure 8. Effect of control cylinder position on CL and CD.

Influence of two-cylinder positioning on the coefficients CL and CD

Figure 9 shows the evolution of CL and CD coefficients according to the location of the two cylinders on the profile NACA2415. The optimal position of the second cylinder at 15 % of the chord C, gives a CL increase of 74.15 % and a CD decrease of 12.98 %. We acknowledge a significant decrease in lift and drag at 0.45C position, due to the abrupt increase in stall at this location, according to literature, asymmetric aerodynamic profiles at AOA zero-degree (0°), record the stall at 40 % of the chord. Figure 9 clearly shows that the first configuration gives very satisfactory results.

Figure 10 shows a comparison of CL and CD evolution of typical configurations (i, ii) with basic NACA2415 profile.

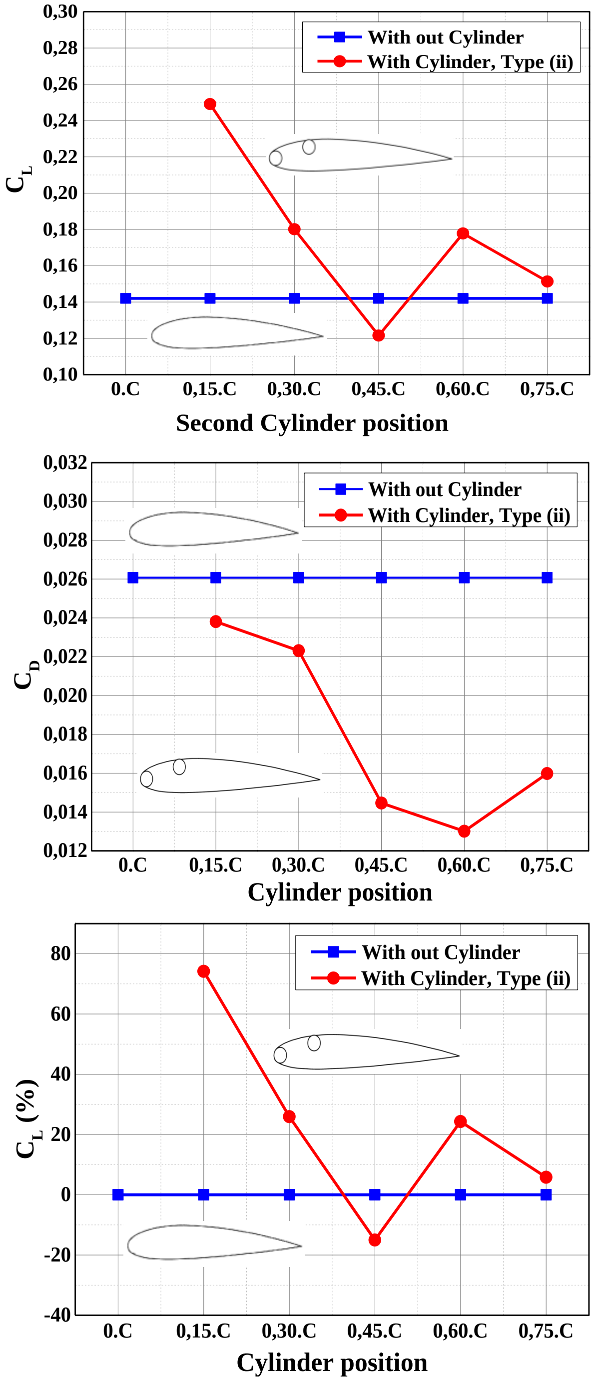

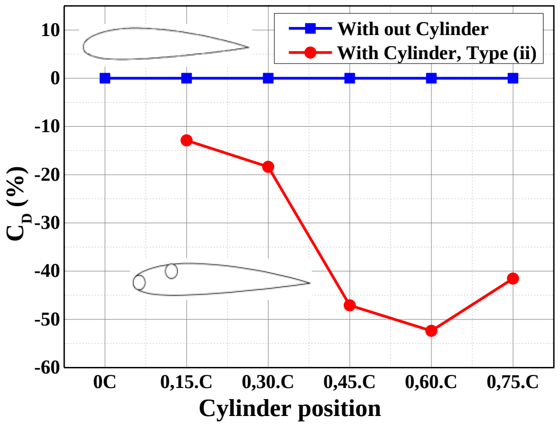

Figure 9. Effect of second cylinder position on CL and CD.

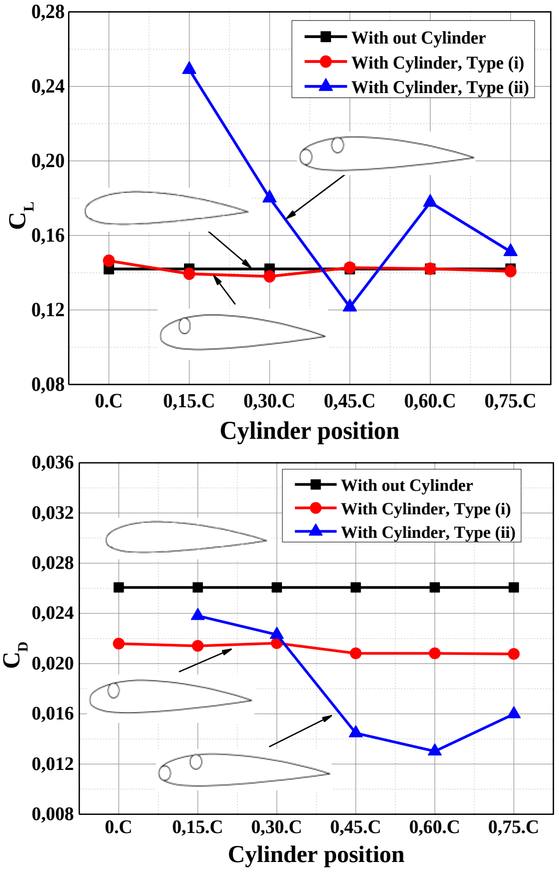

Figure 10. Effect of the position of rotating cylinders in different configurations on CL and CD.

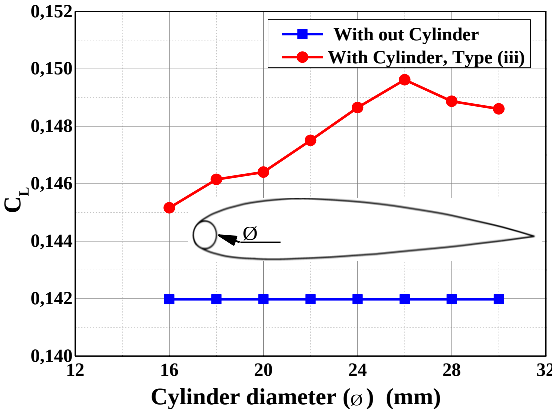

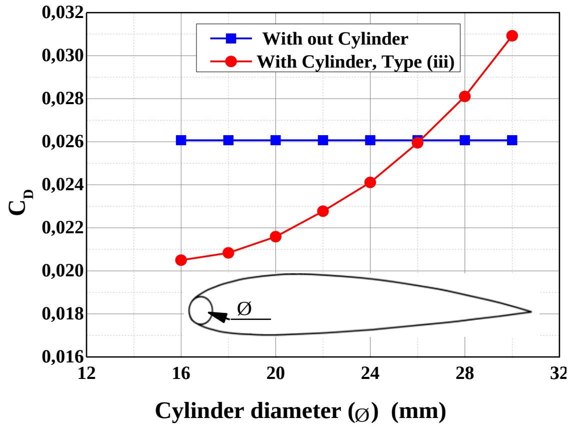

Figure 11. Effect of rotating cylinder diameter on CD and CL.

The influence of cylinder diameter variation on coefficients CL and CD

Based on the results obtained in the first part of this study, the cylinder positioned at the leading-edge, has a varying diameter ∅ at 16, 18, 20, 22, 24, 26, 28, and 30 mm. Figure 11 shows the evolution of CL and CD coefficients according to the diameter. The increased diameter positively affects the CL and CD.

The two parameters indicate an increase in proportion with the increase in diameter of the rotating cylinder until ∅ = 26 mm, and we observe the decrease in CL, as for the contained increase in CD.

CONCLUSION

The study is a numerical investigation of turbulent flow around an aerodynamic profile NACA 2415 equipped with rotating cylinder(s) at positions determined in parallel to the upper-surface, and allows to conclude the following:

- Equipping the aerodynamic profile NACA2415 with a rotating cylinder at the leading-edge gives the best result, it increases the CL by about 3 % and decreases CD by about 17 %, the other positions along the profile give only satisfaction for drag.
- Equipping the aerodynamic profile NACA2415 with two cylinders, the first cylinder at the leading-edge and the second cylinder at 15 % of the chord C, gives 74.15 % increase in CL and a 12.98 % decrease in CD; the other configurations are less important.
- A relatively proportional relationship between the variations of the rotating cylinder diameter positioned at the leading-edge of the aerodynamic profile NACA2415 and coefficients CL and CD, are kept up to the level where the diameter of the cylinder counterbalances the thickness of the profile.

Nomenclature

AOA - angle of attack
ω - cylinder angular velocity (rad/s)
C - profile chord
∅ - cylinder diameter (m)
CL - coefficient of lift
P - pressure (N/m^2), (Pa)
CD - coefficient of drag
Re - Reynolds number
D - distance between leading-edge and cylinder centre

Φ - cylinder rotational speeds (V_C/V)
V - flow velocity of the fluid (m/s)
$k\varepsilon$ - turbulence model
V_C - linear cylinder speed (m/s)

REFERENCES

1. Wanhill, R. (2009), *Some notable aircraft service failures investigated by the National Aerospace Laboratory (NLR)*, Struct. Integ. Life, 9(2): 71-87.
2. Fekaouni, M.F., Maspeyrot, P., Hadj Meliani, M., Youcefi, A. (2019), *Passive structural control of model car drag by transverse separating plates*, Struct. Integ. Life, 19(1): 37-44.
3. Prince, S.A., Khodagolian, V., Singh, C., Kokkalis, T. (2009), *Aerodynamic stall suppression on airfoil sections using passive air-jet vortex generators*, AIAA J, 47(9): 2232-2242. doi: 10.2514/1.41986
4. Aziz, M.A.B., Islam, M.S. (2017), *Effect of lower surface modification on aerodynamic characteristics of an airfoil*, In: Proc. of Int. Conf. on Mech. Eng. and Renewable Energy (ICMERE 2017-PI-250), Chittagong, Bangladesh, 2017.
5. Rahman, M., Hossain, M.A., Uddin, M.N., Mashud, M. (2015), *Experimental study of passive flow separation control over NACA 0012 airfoil*, In: Proc. of Int. Conf. on Mech. Eng. and Renewable Energy (ICMERE2015-PI-233), Chittagong, Bangladesh, 2015.
6. Butt, F.R., Talha, T. (2019), *Numerical investigation of the effect of leading-edge tubercles on propeller performance*, J Aircraft, 56(3): 1014-1028. doi: 10.2514/1.C034845
7. Butt, F.R., Talha, T. (2018), *A parametric study of the effect of the leading-edge tubercles geometry on the performance of aeronautic propeller using computational fluid dynamics (CFD)*, In: Proc. of the World Congress on Engineering, 2018, Vol.II WCE 2018, London, U.K.
8. Pfeiffer, N.J. (2018), *Slotted airfoil with control surface*, AIAA Aviation Forum, Applied Aerodynamics Conference, Atlanta, Georgia, 2018. doi: 10.2514/6.2018-3958
9. Hariyadi, S. Sutardi, S., Widodo, W. (2019), *Numerical analysis of the Reynolds number effect on the aerodynamic performance wing airfoil Eppler 562 with wingtip fence*, J Phys.: Conf. Ser. 1381(1): 012055. doi: 10.1088/1742-6596/1381/1/012055
10. Nechad, S., Khelil, A., Hadj Meliani, M., et al. (2018), *Three-dimensional numerical investigation on swirling jets and elliptic jets with different aspect ratio*, Struct. Integ. Life, 18(3): 197-205.
11. Benard, N., Jolibois, J., Moreau, E. (2009), *Lift and drag performances of an axisymmetric airfoil controlled by plasma actuator*, J Eletrostat. 67(2-3): 133-139. doi: 10.1016/j.elstat.2009.01.008
12. You, D., Moin, P. (2008), *Active control of flow separation over an airfoil using synthetic jets*, J Fluids Struct. 24(8): 1349-1357. doi: 10.1016/j.jfluidstructs.2008.06.017
13. Fournier, G., Pellerin, S., Phuoc, L.T. (2005), *Contrôle par rotation ou par aspiration de l'écoulement autour d'un cylindre calculé par Simulation des Grandes Échelles (Control by rotation or by boundary layer suction of the flow around a circular cylinder by using Large Eddy Simulation)*, C.R. Mecanique 333(3): 273-278. doi: 10.1016/j.crme.2004.11.001
14. Sharma, A. Mishra, T., Chalia, S., Naagar, M. (2018), *Subsonic flow study and analysis on rotating cylinder airfoil*, Int. Res. J Eng. Technol. (IRJET), 05(06): 1009-1014.
15. Asrokin, A., Ramly, M. R., Ahmad, A.H. (2013), *Rotating cylinder design as a lifting generator*, 2nd Int. Conf. on Mech. Eng. Res. (ICMER 2013), IOP Conf. Series: Mater. Sci. Eng. 50: 012025. doi: 10.1088/1757-899X/50/1/012025
16. Tokumaru, P.T. Dimotakis, P.E. (1993), *The lift of a cylinder executing rotary motions in a uniform flow*, J Fluid Mech. 255: 1-10. doi: 10.1017/S0022112093002368
17. Modi, V.J., Yokomizo, T. (1994), *On the boundary-layer control through momentum injection: Studies with applications*, Sadhana, 19(Part 3): 401-426. doi: 10.1007/BF02812162
18. Ramlan, I., Darlis, N., Ishak, I.A., et al. (2019), *Comparison between Solidworks and Ansys CFX flow simulation on aerodynamic studies*, J Complex Flow, 1(2): 26-30.